A 3D Numerical Model to Estimate Lightning Types for PyroCb Thundercloud

Surajit Das Barman , Rakibuzzaman Shah , Syed Islam , Apurv Kumar *

Posted Date: 2 May 2024

doi: 10.20944/preprints202405.0112.v1

Keywords: cloud-to-ground lightning; lower positive charge structure; pyrocumulonimbus; surface charge density; tripole thundercloud

Article

A 3D Numerical Model to Estimate Lightning Types for PyroCb Thundercloud

Surajit Das Barman †,‡, Rakibuzzaman Shah, Syed Islam and Apurv Kumar *,‡

Centre of New Energy Transition Research, Federation University Australia;
surajitdasbarman@students.federation.edu.au, m.shah@federation.edu.au, s.islam@federation.edu.au
* Correspondence: apurv.kumar@federation.edu.au
† Current address: Federation University Australia, Mt Helen, Ballarat VIC 3353, Australia.
‡ These authors contributed equally to this work.

Abstract: Pyrocumulonimbus (pyroCb) thunderclouds, produced from extreme bushfires, can initiate frequent cloud-to-ground (CG) lightning strikes containing extended continuing currents. This, in turn, can ignite new spotfires and inflict massive harm on the environment and infrastructures. This study presents a 3D numerical thundercloud model for estimating the lightning of different types and its striking zone for the conceptual tripole thundercloud structure which is theorized to produce the lightning phenomenon in pyroCb storms. More emphasis is given to the lower positive charge layer, and the impacts of strong wind shear are also explored to thoroughly examine various electrical parameters including the longitudinal electric field, electric potential, and surface charge density. The simulation outcomes on pyroCb thunderclouds with a tripole structure confirm the presence of negative longitudinal electric field initiation at the cloud's lower region. This initiation is accompanied by enhancing the lower positive charge region, resulting in an overall positive electric potential increase. Consequently, negative surface charge density appears underneath the pyroCb thundercloud which has the potential to induce positive cloud-to-ground (+CG) lightning flashes. With wind shear extension of upper charge layers in pyroCb, the lightning initiation potential becomes negative to reduce the absolute field value and would generate -CG lightning flashes. The suggested model would establish the basis for identifying the potential area impacted by lightning and could also be expanded to analyze the dangerous conditions that may arise in wind energy farms or power substations in times of severe pyroCb events.

Keywords: cloud-to-ground lightning; lower positive charge structure; pyrocumulonimbus; surface charge density; tripole thundercloud

1. Introduction

Pyrocumulonimbus (pyroCb) thunderclouds commonly form above bushfires, expanding to substantial heights and influencing the chemical composition as well as the concentrations of aerosol in the upper part of the troposphere [1]. In the formation of pyroCb thunderstorms, the presence of aerosol particles produced by smoke serves as cloud condensation nuclei (CCN), exerting a significant influence on the advancement of the storms. One of the most crucial impacts of pyroCb is the initiation of additional wildfires by cloud-to-ground (CG) lightning. Similar to conventional thunderclouds, pyroCb clouds can result in both positive and negative cloud-to-ground (+CG and -CG) lightning, with +CG being more likely to trigger secondary spot fires and cause extensive harm to nature [1–3].

Over 90% of all lightning strikes are of negative polarity which is frequently observed in thunderstorms that occur in humid conditions. Conversely, +CG strikes are often observed in dry environments with higher cloud bases [4]. These +CG flashes also occur in thunderstorms such as pyroCb, which release significant amounts of smoke into the atmosphere [5]. Multiple investigations have shown that CG strokes of either positive or negative having large continuous currents could start most of the fires [2,6–8]. The emergence of secondary bushfires ignited by CG lightning has become a significant concern for firefighting management on a global scale. Although there has been a notable

 doi:10.20944/preprints202405.0112.v1

rise in the number of pyroCb events in literature, only a few investigations have been conducted in recent years. Over the period of 1973-2020, the southeastern part of Australia faced a number of distinct pyroCb storms that generated a large number of lightning strikes to start the new spot fires and enhanced the longevity of the pyroCb storms [9,10]. These fires were exacerbated by several consecutive days of unprecedented high temperatures and dry weather conditions. In August 2013, Western North America experienced the occurrence of 88 massive wildfires, which gave rise to 26 highly intense pyroCb storms [11].

Numerous studies in the past have investigated the electrical conditions that promote the formation of CG lightning strikes could serve as a crucial indicator for understanding specific phenomena associated with pyroCb events. Multiple hypotheses have been developed recently to explain the electrical configurations of charge regions and situations that result in both -CG and +CG lightning strikes and their association with thunderstorms [12,13]. The overall charge distribution of the conventional thundercloud developed in a moist environment is commonly visualized as a vertical tripole having three charge layers: a predominantly positive layer at the upper portion, a dominant negative layer in the middle, and an auxiliary positive layer below the main negative, typically of smaller magnitude [15]. This lower positive charge layer, in particular, has a crucial role in generating -CG flashes [16,17]. On the other hand, the presence of an enlarged region of positive charge at the bottom of thunderclouds may begin the progression of positive downward leaders to initiate +CG strikes [13,17,18,30,31]. Therefore, there has been considerable focus recently on the specific significance of the lower positive charge region. To date, there has been no literature work on the distribution of charges or investigations into the electrical circumstances conducive to lightning discharges in pyroCb events. The conditions present in pyroCb storms, characterized by strong wind shear and undiluted updrafts, increase the likelihood of exhibiting tripole charge structure while forming pyroCb thunderclouds [9,11]. Certain studies consider the tilted tripole charge structure in severe thunderstorms, where the charge centers in the upper cloud region are shifted towards the direction of the strong wind shear [21,22]. This displacement can separate the positive and negative charge regions, allowing both +CG/-CG flashes to occur from the displaced positive charge region.

In recent years, a method widely used to develop and understand thundercloud charge structures is the physical thundercloud model which incorporates several complex factors, including induced electric charge, the state of lightning leaders, and the formation of corona regions [26–28]. For analyzing the actual thunderstorm process at the mirco-physical level, this method highly relies on observation data which makes it computationally expensive over large-scale domains. Nowadays, the numerical thundercloud model coupled with the empirical governing equations become widely popular in studying the configuration and dynamics of thunderclouds [16,19–22]. This stochastic model based on electrostatic concepts presents the cloud model in an axisymmetric manner, employing the non-inductive charging approach to describe the electrification of the thundercloud. Although this modeling technique is complex and requires significant time, it is remarkably efficient in capturing the dynamic evolution of a thundercloud that could be useful to identify the precise locations on Earth's surface or any object in danger due to thunder or lightning.

In this paper, a 3-D stochastic thundercloud model is demonstrated to simulate the conceptual tripole cloud structure, which is proposed as a representation of a pyroCb thundercloud. More attention is placed on the lower positive charge layer to conduct a comprehensive analysis of different electric states that benefit CG flash generations. In addition, the behavior of the pyroCb thundercloud under strong wind shear is investigated. The suggested model demonstrates how alteration in the size and intensity of the charge layers can impact both thundercloud potential and field distributions, along with surface charge density. This analysis can be valuable in understanding and predicting the occurrence of lightning flashes of different types and their striking zones.

 doi:10.20944/preprints202405.0112.v1

2. Thundercloud Model Description

The main aim of this paper is to explain the electric states in a pyroCb thundercloud that favor the generation of CG flashes of different types, depending on its charge structure. For modeling, the conventional tripole charge structure contains a negative screening layer (SC) at the top, along with upper positive (UP), middle negative (MN), and lower positive (LP) layers are considered to represent the pyroCb thundercloud. For straightforward visualization, a vertical cross-sectional view (in xz plane) of the conceptual tripole structure based pyroCb thundercloud is depicted in Figure 1(a). The x-axis represents the horizontal dimension of the Earth's surface beneath the thundercloud, while the z-axis corresponds to the vertical extent of the charged region. To simplify the analysis, the permittivity in the atmospheric region above z is considered to be the same as that of a vacuum. Typically, the charge magnitude of both UP and MN charge layers ranges from tens to hundreds of coulombs. The LP charge region which is located below the freezing level (a few km above the ground surface) is generally thought to be responsible for increasing the field magnitude at the bottom of the MN charge layer and initiating -CG lighting leader toward the ground [20]. The exact position of the LP charge region is highly influenced by factors such as the season and latitude. This tripole charge configuration in pyroCb can be influenced by the intense and undiluted updrafts in case of severe wildfire events, enhancing the LP charge to overpower the MN charge layer. This disruption can impact the lightning types (either +CG or -CG) produced by the pyroCb thundercloud and its striking locations on the ground. Another atmospheric complex factor known as the vertical wind shear can cause the main positive change region at the top to shift towards the thundercloud's forward flank as shown in Figure 1(b). The absence of a negative charge region no longer provides shielding for the positive charge region. As a result, a +CG flash can now originate directly from the displaced positive charge region. In Figure 1(b), parameter d represents the difference between the initial and present position of the extended boundary on the right side of the UP and SC charge layers.

 doi:10.20944/preprints202405.0112.v1

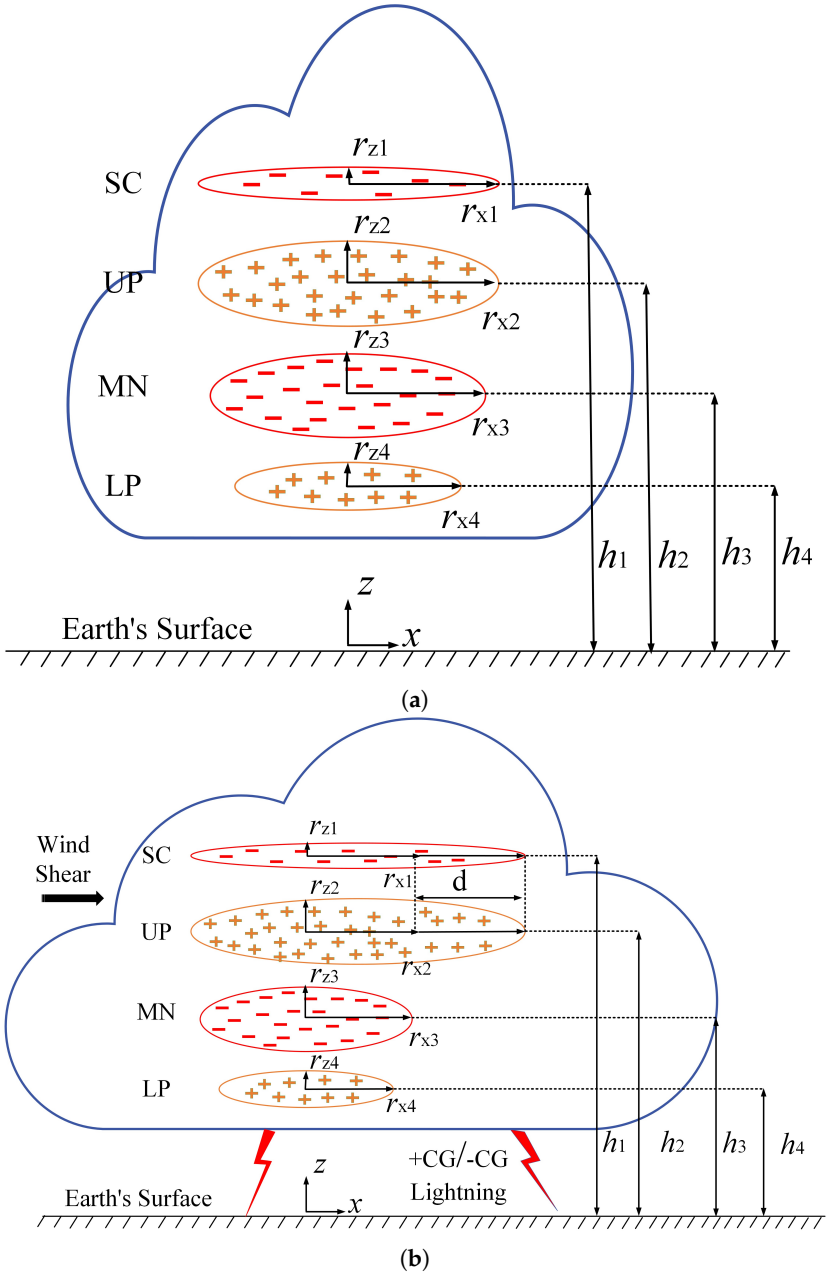

Figure 1. PyroCb thundercloud exhibits: (a) a tripole structure characterized by a prevailing upper positive (UP) charge layer, a prominent middle negative (MN) and a minor lower positive (LP) charge layers, accompanied by an extra negative screening layer (SC) positioned at the top, (b) effect of wind-shear to create the titled structure.

The proposed tripole structure based pyroCb model is built in 3D, using a 30 km $\times$ 30 km $\times$ 30 km cartesian domain. This simulation domain is discretized using 61 $\times$ 61 $\times$ 61 equidistant node points by keeping the distance between the neighboring points along three axes equal. For modeling, each charge region is regarded as having an elliptical shape with a proportional charge density. This relationship can be demonstrated by (1) below, which states the characteristics of the distribution.

$$\rho_n(x,y,z) = \rho_n(0) exp\left[\frac{(x-x_{0n})^2}{{r_{xn}}^2} + \frac{(y-y_{0n})^2}{{r_{yn}}^2} + \frac{(z-h_n)^2}{{r_{zn}}^2}\right] \quad (1)$$

 doi:10.20944/preprints202405.0112.v1

where $\rho_n(0)$ denotes the amplitude of maximum charge density of nth charge layer with $n = 1, 2, 3, ...$; x_{0n} and y_{0n} act for representing the lateral center of nth charge layer, and h_n determine its corresponding altitude. Parameters r_{xn} and r_{yn} define the corresponding lateral extents in both x and y directions while r_{zn} presents the vertical range in the z-axis. Two different configurations for the tripole charge structure are provided in Table 1, with the magnitude of LP charge in the 2nd configuration extended from 18 C to 30 C. The vertical range and lateral extents are enhanced from 1 km to 1.2 km and from 3 km to 4 km, respectively in the 2nd configuration. The electrical and dimensional parameters of each charge region are derived from the studies documented in [20,21]. Based on the satellite data, the average cloud-base heights of pyrocumulonimbus (pyroCb) clouds ranged from 3 to 5 km. These values differ by approximately 7% compared to the simulated data reported in [23]. In this model, the cloud-base height of tripole structure based pyroCb thunderclouds is represented by the altitude of its lower charge layers estimated from the ground surface.

Table 1. Parameters related to the dimensions and electrical properties of tripole structured pyroCb thundercloud.

Config.	Charge Layer	Altitude, h_n (km)	Lateral range, r_x & r_y (km)	Vertical range, r_z (km)	Lateral centre, x_0 & y_0 (km)	Charge Density, ρ (nC/m^3)	Charge, Q (C)
1	SC	11.75	6	0.5	15	-1.1	-19
	UP	9.75	6	1.5	15	2.2	77
	MN	6.75	5	1.5	15	-2.5	-73
	LP	4.25	3	1	15	1.0	18
2	SC	11.75	6	0.5	15	-1.1	-19
	UP	9.75	6	1.5	15	2.2	77
	MN	6.75	5	1.5	15	-2.5	-73
	LP	4.25	4	1.2	15	1.5	30

To model the impact of wind shear extension on tripole structure in pyroCb, the positioning and lateral extents of both SC and UP charge layers are consistently adapted while keeping their left boundary fixed. The electrical charge within the anvil section of the pyroCb is assumed to have initially formed within the central region of the thundercloud and subsequently moved towards the forward flank due to lateral air currents originating from the electrified area. Throughout this adjustment, the extension parameter d has been changed by 2, 4, and 8 km while the charge distribution within the upper thundercloud regions remains unchanged. The simulation assumes the ground surface (positioned at $x = 0$ and $y = 0$) beneath the pyroCb thundercloud as an unconstrained conducting plane with uniform potential. Electric potential, denoted as $V(x, y, z)$ produced by nth charge region in the thundercloud represented by their respective charge density $\rho_n(x, y, z)$ can be determined by solving the Poisson equation:

$$\nabla^2 V = -\frac{\rho_n(x, y, z)}{\epsilon_0} \tag{2}$$

where, ϵ_0 represents the free space's permittivity. In computational terms, the total potential for the pyroCb thundercloud can be achieved by combining the influences from all individual nodes (i, j, k) within the computational domain, along with their along with their respective reflections or images given in (3).

$$V_{i,j,k}{}^{(m)} = V_{i,j,k}{}^{(m-1)} + \omega \Big[A(V_{i+1,j,k}{}^{(m-1)} + V_{i-1,j,k}{}^{(m)}) + B(V_{i,j+1,k}{}^{(m-1)} + V_{i,j-1,k}{}^{(m)}) + C(V_{i,j,k+1}{}^{(m-1)} + V_{i,j,k-1}{}^{(m)}) + \frac{D}{\epsilon_0} \sum_n \rho_n(x, y, z) \Big] \tag{3}$$

where,

$$A = \frac{\delta y^2 \delta z^2}{2(\delta x^2 \delta y^2 + \delta y^2 \delta z^2 + \delta x^2 \delta z^2)}$$

$$B = \frac{\delta x^2 \delta z^2}{2(\delta x^2 \delta y^2 + \delta y^2 \delta z^2 + \delta x^2 \delta z^2)}$$

 doi:10.20944/preprints202405.0112.v1

$$C = \frac{\delta x^2 \delta y^2}{2(\delta x^2 \delta y^2 + \delta y^2 \delta z^2 + \delta x^2 \delta z^2)}$$

$$D = \frac{\delta x^2 \delta y^2 \delta z^2}{2(\delta x^2 \delta y^2 + \delta y^2 \delta z^2 + \delta x^2 \delta z^2)}$$

Here, superscripts (m) and $(m-1)$ represent their respective present and previous iteration cycles. The grid spacing between the neighboring node points along three corresponding axes are presented by δx, δy and δz, respectively. Considering $\delta x = \delta y = \delta z$ in the simulation simplifies the constants A, B, C and D equal to be $1/6$. After every cycle, the electric potential of the entire computational domain was updated by (3) using the successive over-relaxation (SOR) algorithm where the speed of convergence was governed by the relaxation parameter ω. The electric field E of each computational grid can be obtained from V from the expression given in 4,

$$E = -\nabla V \tag{4}$$

The presence of tripole cloud structure in pyroCb thunderstorms significantly affects the charge distribution on the ground surface, especially with the dominant MN charge leading to the repulsion of negative charges on the ground. As a result, the ground surface or any object underneath the pyroCb thundercloud acquires positive charges. As the intensity of the LP charge layer increases, it initiates the repulsion of positive charges present on the ground surface. This repulsion stops the downward movement of the negative leader, impending its progression. The value of the surface charge density that appears on the ground $(x, y \to 0)$ can be computed by (5).

$$\sigma = -\epsilon_o \frac{\partial}{\partial z} V \Big|_{x=0, y=0} \tag{5}$$

3. Simulation Results and Discussion

3.1. Tripole Structure with Large Lower Positive Charge

To investigate whether a large LP charge region affects the electrical conditions to generate CG lightning, simulations are carried out on two different configurations of pyroCb thundercloud with a tripole structure. Figure 2(a1-a2) illustrates the cross-sectional view of the simulated tripole charge configurations. These charge configurations are built at the midpoint of the y-axis within the computational space, specifically along the xz plane. The electric potential generated by the tripole structure and their field distribution are analyzed and illustrated in Figure 2(b1-b2) and Figure 2(c1-c2), respectively. When the LP charge region of the pyroCb thundercloud gets enhanced in 2^{nd} configuration (Figure 2(a2)), the overall potential of the pyroCb thundercloud shows a positive increment compared to its 1^{st} configuration depicted in Figure 2(b2). With a relatively large LP charge, the magnitude of the electric field within the thundercloud decreases as evident in Figure 2(c2) in comparison to Figure 2(c1). This observation aligns with the characteristics dictated by the law of the electrostatic field.

$$E_{th}(z) = \pm 201.7 exp\left(-\frac{z}{8.4}\right) \tag{6}$$

 doi:10.20944/preprints202405.0112.v1

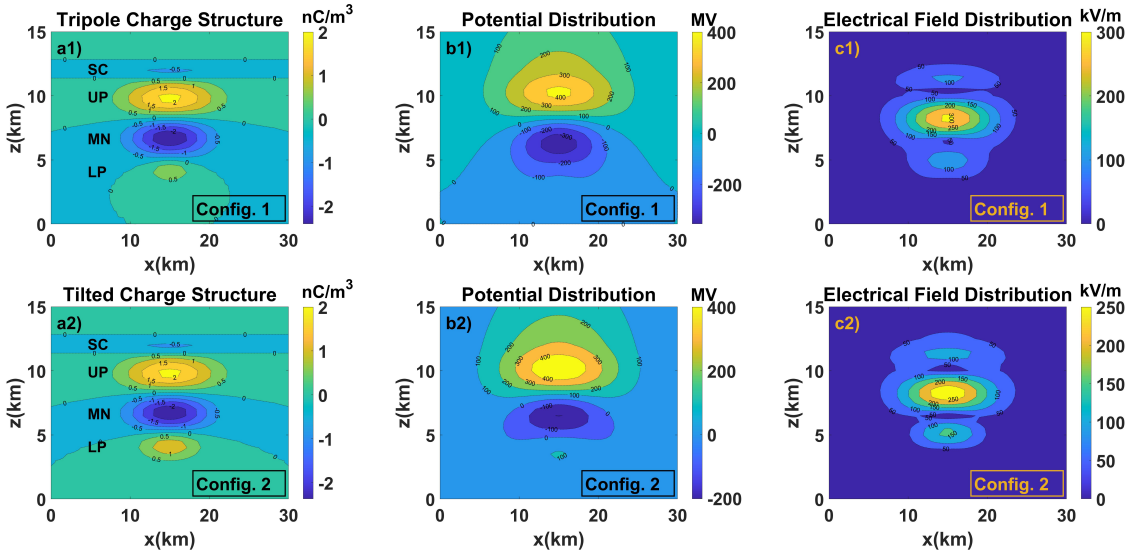

Figure 2. The vertical profile of the pyroCb thundercloud model (in xz plane) exhibits a tripole charge structure under two different conditions: (a1) without LP charge enhancement (configuration 1) and (a2) with increased LP charge region (configuration 2). The depictions include the corresponding distributions of electric potential (b1-b2) and the changes in electric field (c1-c2).

Illustrating two distinct configurations of the pyroCb thundercloud, Figure 3(a1-a2) and Figure 3(b1-b2) display the projected electric potential values at the maximum field and longitudinal electric field, respectively. These are measured along the z axis at the core (at $x = 15$ km and $y = 15$ km) of the simulation domain. In Figure 3(a1-a2), the symbol "x" denotes the particular node point where the maximum electric field with discharge initiation occurs. The mathematical expression in 6 [24] represents the relationship between altitude z and the initiation threshold value $E_{th}(z)$, marked as red dotted lines in Figure 3(b1-b2). As observed in Figure 3(a1-a2), the maximum potential shows gradual incremental trends while the minimum potential decreases when the LP charge region is enhanced. At the same time, the lightning flash initiation point of the pyroCb thundercloud has shifted from -51.73 MV (in 1^{st} configuration) to a positive value of 203.397 MV in 2^{nd} configuration. This analysis agrees with the findings reported in [25], which indicate that the CG lightning initiation (regardless of their polarity) occurs only when the absolute potential value at the initiation point is significantly higher than 0 MV. In contrast to 1^{st} configuration, the longitudinal electric field (E_z) at the thundercloud bottom exhibits a negative shift with the increase of LP charge layer (Figure 3(b2)).

Preprints.org (www.preprints.org) | NOT PEER-REVIEWED | Posted: 2 May 2024 doi:10.20944/preprints202405.0112.v1

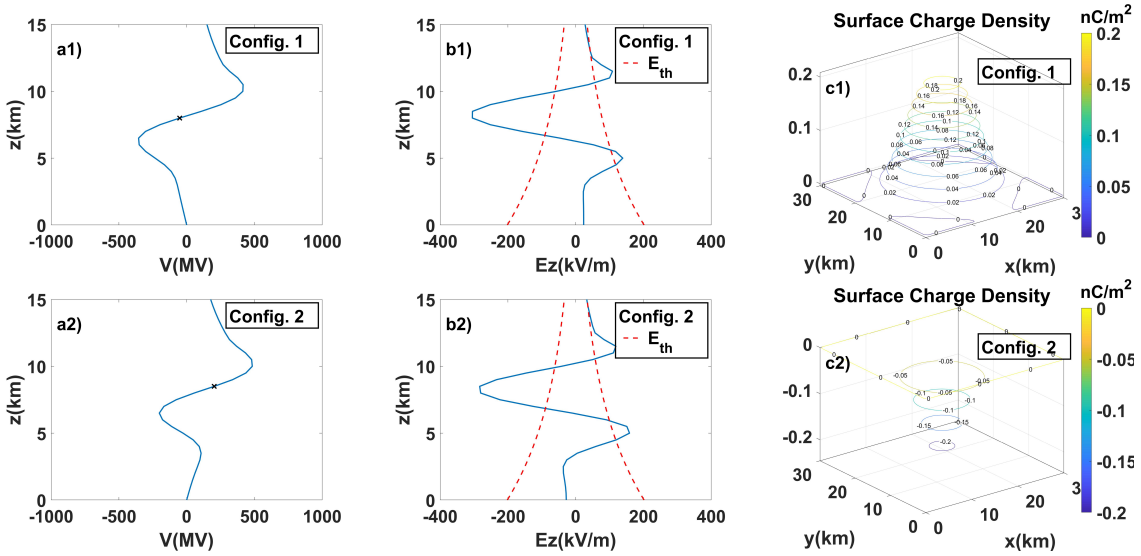

Figure 3. Graphs depicting the electric potential V(MV), are shown at the point of maximum field where the initiation of flash is marked with an "x" (a1-a2). The longitudinal electric field E_z(kV/m) and surface charge density σ for two different thundercloud configurations are also illustrated in (b1-b2) and (c1-c2), respectively.

Table 2 presents the outcomes of surface charge density σ for simulated pyroCb thundercloud. The table also indicates the probable lightning types associated with two distinct tripole charge setups. As observed in 1^{st} configuration (Figure 3(C1)), surface charge density σ becomes positive within the range $3.5 \leq x \leq 26.5$ km and $3.5 \leq y \leq 26.5$ km on the projected ground surface beneath the pyroCb thundercloud. This would trigger the start of -CG flashes. This corresponds to the theory that attributes the presence of LP charge layer below the pyroCb thundercloud amplifies the electric field and triggers -CG flashes [12,17]. A similar simulation for σ is carried out for the 2^{nd} configuration of the pyroCb thundercloud by enlarging the lateral and vertical extents of LP charge region, along with adjusting its charge magnitude. As depicted in Figure 3(C2), the value of σ turns negative across the entire simulation domain, reaching its peak of 0.2454 nC/m^2 at the thundercloud's core. This simulated negative peak is larger in magnitude than the maximum value of σ (0.2087 nC/m^2 at x = 14, $14.5 \leq y \leq 15.5$ km) appeared in the 1^{st} configuration of the pyroCb thundercloud. The negative value of σ in 2^{nd} configuration could trigger the initiation of a downward positive leader, ultimately causing a +CG flash to form as it reaches the ground. These projected outcomes align with the findings in [20], which concluded that the existence of a large LP charge layer hinders negative lightning leader progression to the ground. Consequently, this terminates the incidence of -CG flashes while raising the likelihood of positive +CG lightning. This phenomenon takes place when a negative electric field other than a positive or zero value appears at the thundercloud's bottom.

Table 2. Possible Lightning Categories for Simulated PyroCb Thundercloud with Tripole Charge Configuration.

r_x and r_y of LP (km)	r_z of LP (km)	Charge of LP (C)	Range of x and y (km)	Polarity of σ	Peak Value of σ (nC/m^2)	Probable Lightning Types
3	1	18	$3.5 \leq x \leq 26.5$ km, $3.5 \leq y \leq 26.5$ km	Positive	0.2087 nC/m^2 at x = 14, $14.5 \leq y \leq 15.5$ km	-CG
4	1.2	30	$0 \leq x, y \leq 30$ km	Negative	0.2454 nC/m^2 at x, y = 15 km	+CG

3.2. Impact of wind shear on pyroCb thundercloud

To examine the consequences of wind shear on a pyroCb thundercloud and how the displacement of its charge layers influences potential lightning strike areas, the parameters x_{0n} and r_{xn} of both SC and UP charge layers are altered while keeping MN and LP charge structure same as of configuration 2 in Table 1. The vertical cross-sectional view in Figure 4 illustrates how strong wind shear

 doi:10.20944/preprints202405.0112.v1

displaced the charge layers in pyroCb thundercloud, causing an impact on the overall distribution of thundercloud-generated potential and electric field. In Figure 4(a1-a3), the extension parameter d is varied by 2, 4, and 8 km, respectively while maintaining the value of $\rho_n(0)$ constant to ensure the overall charge of the effected charge regions remains constant. With the wind shear extension in the SC and UP regions, there is observed growth of negative potential, particularly in the middle region of the pyroCb thundercloud, as depicted in Figure 4(b1-b3). Furthermore, the magnitude of the electric field (Figure 4(c1-c3)) within the thundercloud decreases with the rightward lateral extension of SC and UP charge layers, aligning with the principles of the electrostatic field.

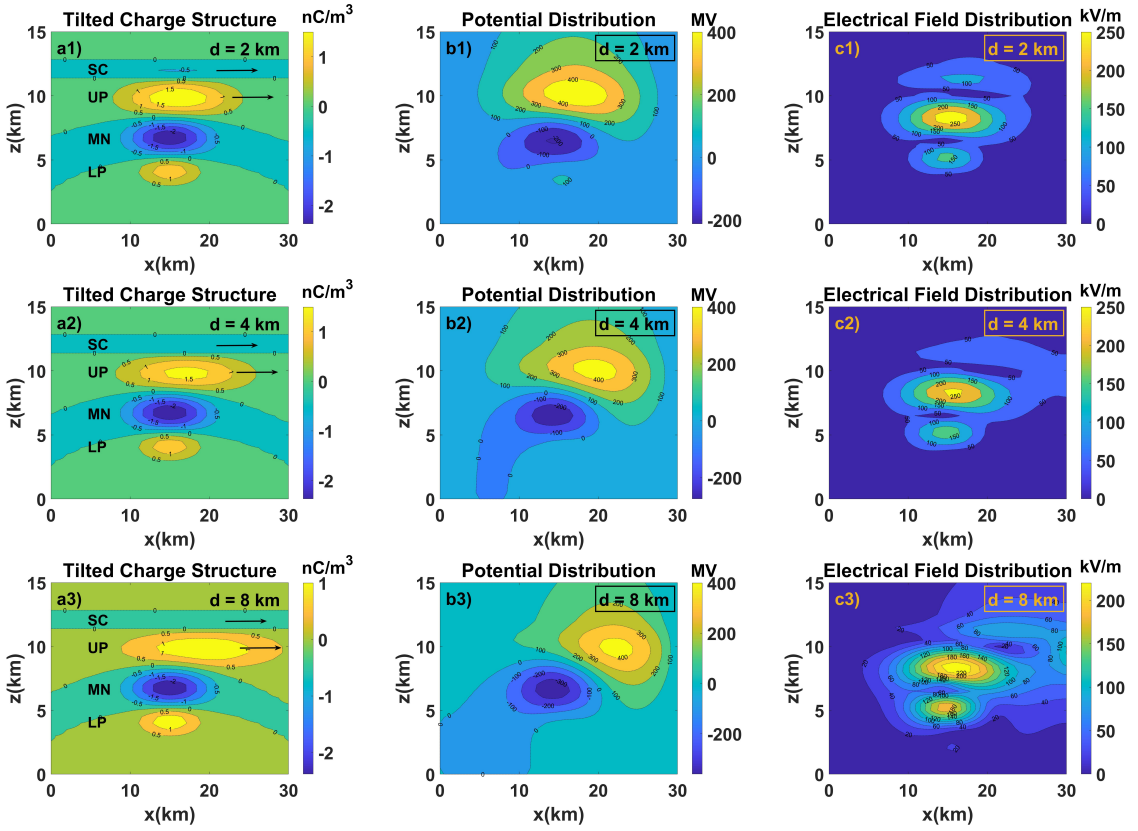

Figure 4. Vertical cross-sectional representation of pyroCb thundercloud incorporating the wind-shear extension of SC and UP charge layers when (a1) $d = 2$, (a2) $d = 4$, and (a3) $d = 8$ km, respectively, and corresponding simulated potential (b1-b3) and electric field (c1-c3) distributions.

Figure 5(a1-a3) and Figure 5(b1-b3) depict the variations in the electric potential V (measured at maximum field point) and longitudinal electrical field E_z at thundercloud core with the effect of wind shear extension. Figure 5(a1-a3) shows that as the UP charge layer shifts horizontally, the maximum potential decreases gradually, whereas the minimum potential experiences a concurrent rise. Consequently, the point at which discharge initiation occurs shifts negatively. The potential at the initiation point of the lightning flash is 178.81 MV for $d = 2$ km as seen in Figure 5(a1). Then, a noticeable change in the potential value at the point of flash initiation becomes evident with an increase in the value of d and ends up at -64.07 MV for $d = 8$ km (Figure 5(a3)). Moreover, the extension of wind shear leads to a reduction in the absolute peak value of the vertical field at the top, while it increases the absolute peak value of the vertical field at the bottom of the pyroCb thundercloud as observed in Figure 5(b1-b3). For various values of extension parameter d, the fluctuations in the simulated surface charge density σ on the ground surface beneath the pyroCb thundercloud are illustrated in Figure 5(c1-c3). The probable lightning types based on the polarity of simulated σ and their identified locations on the ground surface are summarized in Table 3. When $d = 2$ km, the value of σ remains negative over the simulation domain having an absolute peak value of 0.2531 nC/m^2 which is higher

 doi:10.20944/preprints202405.0112.v1

than the peak value measured for the configuration 2 of pyroCb in Table 2. But its location on the ground surface is shifted from 15 km to 15.5 km along the y-axis while remaining fixed at 15 km along the x-axis. For $d \geq 4$ km, the positive value of σ becomes visible for pyroCb, and its absolute peak value is enhanced with increasing values of d, indicating a higher probability of an increase in the -CG flash rate. As indicated in Table 3, the coordinates of the peak negative σ location are notably distant from the center. This spatial distribution suggests that the -CG lightning strikes tend to occur away from the thundercloud core. On the other hand, the absolute peak value of negative σ starts to decrease when $d > 2$ km, with the position slightly shifting away from the core along y direction.

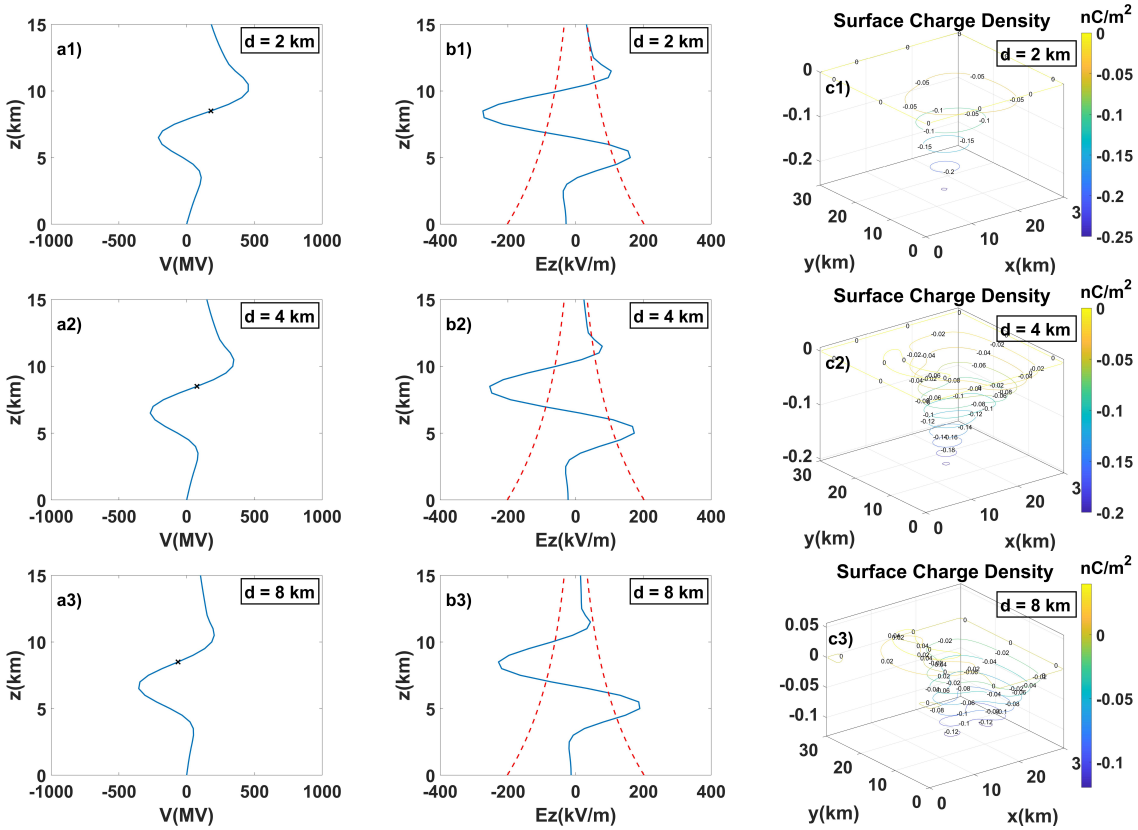

Figure 5. Graphs showing the electric potential V(MV) at maximum field point of pyroCb thundercloud (a1-a3), and its corresponding longitudinal electric field E_z(kV/m) (b1-b3), and surface charge density σ (C1-C3) under the effect of wind-shear.

Table 3. Effect of Wind-shear Extension Leading to Possible Lightning Types in PyroCb Thundercloud.

Extension Parameter, d (km)	Absolute Peak Value of σ (nC/m^2)	Location on Earth's Surface, (x, y) km	Polarity of σ	Probable Lightning Types
2	0.2531	$(15, 15.5)$	Negative	+CG
4	0.0065 0.2035	$(15, 7)$ $(15, 16)$	Positive Negative	-CG +CG
8	0.0565 0.1309	$(13, 8.5)$ $(15, 16.5)$	Positive Negative	-CG +CG

In brief, the objective of this research is to use numerical representation to depict the tripole structure of pyroCb thundercloud and investigate the electrical states of the thundercloud to approximate the probable lightning types and their striking zone on the ground surface. Through the model and simulation, the study has initially revealed the impact of enlarging the lower positive charge layer with the rise in potential and forming negative longitudinal electric field initiation at the thundercloud's bottom. This enlargement leads to a negative surface charge density underneath the pyroCb thundercloud, which can trigger +CG lightning strikes on the ground surface near the core of

 doi:10.20944/preprints202405.0112.v1

the storm. Later, the consequences of the wind-shear extension on the electrical conditions in pyroCb storm is investigated. As seen, the lightning initiation potential shifts to the negative value with the wind shear extension of upper charge regions in pyroCb to reduce the absolute field value and can generate -CG lightning with large lower positive charge. This compact thundercloud model and its quick computational capabilities make it highly valuable for providing early warnings and protection, particularly in the context of pyroCb lightning events caused by wildfires. The proposed work has a high potential to provide a comprehensive explanation of the emergence of different cloud charge structures in pyroCb considering the charging current within the thundercloud and corona near the ground surface.

4. Conclusions

Extreme bushfires can create pyroCb storms that can produce lightning strikes, triggering additional spot fires, and ultimately prolonging the duration of the fire events. Having a comprehensive understanding of pyroCb activity is crucial due to the interplay between the fires and the atmosphere. This can worsen the conditions linked to hazardous fire behavior and may create a significant issue for global firefighting management. This paper demonstrates a 3-D stochastic model for analyzing a pyroCb thundercloud, presumed to exhibit a conceptual tripole charge structure. Initially, the focus has been directed toward the lower positive charge layer of the thundercloud during the process of applying the successive over-relaxation technique to solve Poisson's equation. Afterward, the electrical conditions conducive to +CG/-CG lightnings are investigated, taking into account the horizontal extension of upper charge layers caused by strong wind shear within pyroCb thunderclouds. With this approach, the changes in the flash initiation point, the longitudinal electric field, and the thundercloud's potential have been investigated. Simulation results confirmed the negative longitudinal electric field initiation at the thundercloud's bottom which is accompanied by the enlarged lower positive charge region, ultimately causing a net positive rise in electric potential. The proposed model has demonstrated that adjusting the size and strength of the lower positive charge layer can facilitate the incident of different lightning types during a pyroCb event, depending on the estimated value of surface charge density. This model forms the basis for identifying high-risk zones prone to flashes of lightning in times of extreme weather conditions. Analyzing simulated data of pyroCb thunderclouds would offer crucial insights for evaluating susceptible regions and issuing timely warnings to prevent pyroCb lightning strikes. Such a model can be adapted further to simulate lightning leaders, serving as a foundation for investigating the effects of corona formation and lightning strikes on spinning wind turbines that are impacted by charged particles emitted from pyroCb events.

Author Contributions: Conceptualization, S.D. Barman and A. Kumar; methodology, S.D. Barman; software, S.D. Barman and A. Kumar; validation, R. Shah, S. Islam and A. Kumar; formal analysis, S.D. Barman; investigation, S.D. Barman; resources, S.D. Barman; data curation, S.D. Barman; writing—original draft preparation, S.D. Barman; writing—review and editing, R. Shah, S. Islam and A. Kumar; visualization, S.D. Barman; supervision, R. Shah and A. Kumar; project administration, A. Kumar and R. Shah. All authors have read and agreed to the published version of the manuscript.

Funding: This research received no external funding.

Institutional Review Board Statement: Not applicable.

Informed Consent Statement: Not applicable.

Acknowledgments: We gratefully acknowledge the financial support from the Centre of New Transition Research, Federation University Australia and the Destination Australia scholarship.

Conflicts of Interest: The authors declare no conflicts of interest.

 doi:10.20944/preprints202405.0112.v1

Abbreviations

The following abbreviations are used in this manuscript:

PyroCb	Pyrocumulonimbus
CG	Cloud-to-ground
CCN	Cloud condensation nuclei
SC	Screening layer
UP	Upper positive
MN	Middle negative
LP	Lower positive
SOR	Successive over-relaxation

References

1. Fromm, M.; Lindsey, D.T.; Servranckx, R.; Yue, G.; Trickl, T.; Sica, R.; Doucet, P. and Godin-Beekmann, S. The untold story of pyrocumulonimbus. *Bull. Am. Meteorol. Soc.* **2010**, *91*, 1193–1210.
2. Latham, D. and Williams, E. Lightning and forest fires. *Forest Fires.* **2001**, 375-–418.
3. Ichoku, C.; Giglio, L.; Wooster, M.J. and Remer, L.A. Global characterization of biomass-burning patterns using satellite measurements of fire radiative energy. *Remote Sens. Environ.* **2008**, *112*, 2950-–2962.
4. Carey, L.D. and Buffalo, K.M. Environmental control of cloud-to ground lightning polarity in severe storms. *Mon. Weather Rev.* **2007** *135*, 1327-–1353.
5. Williams, E.; Mushtak, V.; Rosenfeld, D.; Goodman, S. and Boccippio, D. Thermodynamic conditions favorable to superlative thunderstorm updraft, mixed phase microphysics and lightning flash rate. *Atmos. Res.* **2005**, *76*, 288-–306.
6. Tory, K. and Thurston, W. *Pyrocumulonimbus: A literature review*, Bushfire and Natural Hazards CRC: East Melbourne, VIC, Australia, 2015.
7. Rudlosky, S.D. and Fuelberg, H.E. Seasonal, regional, and storm-scale variability of cloud-to-ground lightning characteristics in florida. *Mon. Weather Rev.* **2011**, *139*, 1826-–1843.
8. Xie, Y.; Xu, K.; Zhang, T. and Liu, X. Five-year study of cloud-to-ground lightning activity in yunnan province, china. *Atmos. Res.* **2013**, *129*, 49-–57.
9. Dowdy, A.J.; Fromm, M.D. and McCarthy, N. Pyrocumulonimbus lightning and fire ignition on black saturday in southeast australia. *J. Geophys. Res. Atmos.* **2017**, *122*, 7342-–7354.
10. Deb, P.; Moradkhani, H.; Abbaszadeh, P.; Kiem, A.S.; Engstrom, J.; Keellings, D. and Sharma, A. Causes of the widespread 2019–2020 australian bushfire season. *Earth's Future* **2020**, *8*, e2020EF001671.
11. Peterson, D.A.; Fromm, M.D.; Solbrig, J.E.; Hyer, E.J.; Surratt, M.L. and Campbell, J.R. Detection and inventory of intense pyroconvection in western north america using goes-15 daytime infrared data. *J. Appl. Meteorol. Climatol.* **2017**, *56*, 471—493.
12. Williams, E.R. The electrification of thunderstorms. *Sci. Am.* **1988**, *259*, 88-–99.
13. Nag, A. and Rakov, V.A. Positive lightning: An overview, new observations, and inferences. *J. Geophys. Res. Atmos.* **2012**, *117*, D08109.
14. MacGorman, D.R. and Burgess, D.W. Positive cloud-to-ground lightning in tornadic storms and hailstorms. *Mon. Weather Rev.* **1994**, *122*, 1671-–1697.
15. Williams, E.R. The tripole structure of thunderstorms. *Geophys. Res.* **1989**, *94*, 13151-–13167.
16. Mansell, E.R.; MacGorman, D.R.; Ziegler, C.L. and Straka, J.M. Simulated three-dimensional branched lightning in a numerical thunderstorm model. *J. Geophys. Res. Atmos.* **2002**, *107*, ACL–2.
17. Nag, A., and Rakov, V.A. Some inferences on the role of lower positive charge region in facilitating different types of lightning. *Geophys. Res. Lett.* **2009**, *36*, L05815.
18. Qie, X.S.; Zhang, T.L.; Chen, C.P.; Zhang, G.S.; Zhang, T. and Wei, W.Z. The lower positive charge center and its effect on lightning discharges on the Tibetan Plateau. *Geophys. Res. Lett.* **2005a**, *32*, L05814.
19. Zheng, T.; Tan, Y. and Wang, Y. Numerical simulation to evaluate the effects of upward lightning discharges on thunderstorm electrical parameters. *Adv. Atmos. Sci* . **2021**, *38*, 446—459.
20. Iudin, D.; Rakov, V.; Mareev, E.; Iudin, F.; Syssoev, A. and Davydenko, S. Advanced numerical model of lightning development: Application to studying the role of lpcr in determining lightning type. *J. Geophys. Res. Atmos.* bf217, *122*, 6416-–6430.
21. Wang, H.; Guo, F.; Zhao, T.; Qin, M. and Zhang, L. A numerical study of the positive cloud-to-ground flash from the forward flank of normal polarity thunderstorm. *Atmos. Res.* **2016**, *169*, 183-–190.

22. Barman, S.D.; Shah, R.; Islam, S. and Kumar, A. Numerical Model of Cloud-to-Ground Lightning for PyroCb Thunderstorms. *IEEE J. Sel. Top. Appl. Earth Obs. Remote Sens.* **2023**, *16*, 8689–8701.
23. Lee, S.S.; Kablick III, G.; Li, Z.; Jung, C.H.; Choi, Y.-S.; Um, J. and Choi, W.J. Examination of effects of aerosols on a pyrocb and their dependence on fire intensity and aerosol perturbation. *Atmos. Chem. Phys.* **2020**, *20*, 3357-–3371.
24. Marshall, T.C.; McCarthy, M.P. and Rust, W.D. Electric field magnitudes and lightning initiation in thunderstorms. *J. Geophys. Res. Atmos.* **1995**, *100*, 7097-–7103.
25. Tan, Y.; Tao, S.; Liang, Z. and Zhu, B. Numerical study on the relationship between lightning types and distribution of space charge and electric potential. *J. Geophys. Res. Atmos.* **2014**, *119*, 1003—1014.
26. Cooray, V.; Kumar, U.; Rachidi, F. and Nucci, C.A. On the possible variation of the lightning striking distance as assumed in the iec lightning protection standard as a function of structure height. *Electr. Power Syst. Res.* **2014**, *113*, 79-–87.
27. Mazur V. and Ruhnke, L.H. Model of electric charges in thunderstorms and associated lightning. *J. Geophys. Res. Atmos. 1998*, *103*, 23 299—23 308.
28. Barman, S.D.; Shah, R.; Islam, S.; and Kumar, A. Prediction of Positive Cloud-To-Ground Lightning Striking Zones for Tilted Thundercloud Based on Line Charge Model. In Proceedings of the IEEE PES 14th Asia-Pacific Power and Energy Engineering Conference (APPEEC), Melbourne, Australia, 20-23 November 2022.
29. Tan, Y.;Tao, S.; Liang, Z.; and Zhu, B. Numerical study on relationship between lightning types and distribution of space charge and electric potential. *J. Geophys. Res. Atmos. 2014*, *119*, 1003—1014.
30. Williams, E.R. The electrification of thunderstorms. *Sci. Am. 1988*, *259*, 88-–99.
31. Kong, X.; Zhao, Y.; Zhang, T.; and Wang, H. Optical and electrical characteristics of in-cloud discharge activity and downward leaders in positive cloud-to-ground lightning flashes. *Atmos Res. 2015*, *160*, 28-–38.